

Lithium therapy for human immunodeficiency virus type 1-associated neurocognitive impairment

Giovanni Schifitto,^{1,3} Jianhui Zhong,^{2,3} David Gill,⁴ Derick R Peterson,⁵ Michelle D Gaugh,¹ Tong Zhu,² Madalina Tivarus,³ Kim Cruttenden,¹ Sanjay B Maggirwar,⁶ Howard E Gendelman,⁷ Stephen Dewhurst,⁸ and Harris A Gelbard^{1,8}

Departments of ¹Neurology, ²Biomedical Engineering, ³Imaging Sciences, ⁵Biostatistics and Computational Biology, ⁶Microbiology, and Immunology and ⁸Center for Neural Development and Disease, University of Rochester, Rochester, New York, USA; ⁴Department of Neurology, Pennsylvania State University, Hershey, Pennsylvania, USA; and ⁷Department of Pharmacology and Experimental Neuroscience, University of Nebraska Medical Center, Omaha Nebraska, USA

The objective of this study was to assess lithium safety and tolerability and to explore its impact on cognition, function, and neuroimaging biomarkers in human immunodeficiency virus (HIV)-infected subjects with cognitive impairment. Fifteen cognitively impaired HIV-infected subjects were enrolled in this 10-week open-label study of lithium 300 mg twice daily. Neuroimaging was performed at baseline and following 10 weeks of treatment and included magnetic resonance spectroscopy (MRS), diffusion tensor imaging (DTI), and functional MRI (fMRI). Thirteen of the 14 subjects (93%) that complied with the study visits were able to complete the study on lithium and 11 out of 13 (79%) completed the study at the originally assigned dose of 300 mg twice daily. There were no significant changes in CD4⁺ lymphocyte cell count and plasma HIV RNA. Cognitive performance and depressive mood did not improve significantly after the 10-week lithium treatment; however, neuroimaging revealed a decrease in the glutamate+glutamine (Glx) peak in the frontal gray matter, increased fractional anisotropy, and decreased mean diffusivity in several brain areas, and changes in brain activation patterns, suggestive of improvement. These results suggest that lithium can be used safely in HIV-infected individuals with cognitive impairment. Furthermore, the neuroimaging results suggest that lithium may improve HIV-associated central nervous system (CNS) injury; thus, further investigations of lithium as an adjunctive treatment for HIV-associated cognitive impairment are warranted. *Journal of NeuroVirology* (2009) 15, 176–186.

Keywords: HIV; lithium; cognitive impairment; neuroimaging; fMRI

Introduction

The incidence of human immunodeficiency virus type 1 (HIV-1)-associated neurocognitive disorders

Address correspondence to Giovanni Schifitto, MD, Department of Neurology, Movement & Inherited Neurologic Disorders, Clinical Trials Coordination Center, 1351 Mount Hope Avenue, Suite 223, Rochester, NY 14620, USA. E-mail: giovanni.schifitto@ctcc.rochester.edu.

This study was funded in part by NIH grants P01 MH64570 and R01 MH64409, and by a General Clinical Research Center (GCRC) grant, M01 RR00044, from the National Center for Research Resources, NIH.

Received 30 October 2008; Revised 9 January 2009; accepted 15 January 2009.

(HAND) (Antinori *et al*, 2007) has persisted, with only partial improvements in disease severity despite the use of highly active antiretroviral therapy (HAART) (Sacktor *et al*, 2002). This fact emphasizes that in addition to optimal HAART, there is a need to develop successful adjunctive treatments for this disease. The central pathogenic feature of disease revolves around the secretion and subsequent neurotoxicity of inflammatory mediators from virus-infected and immune competent mononuclear phagocytes (MPs; brain macrophages and microglia) (Glass *et al*, 1993). Cellular-based toxicities acting in concert with viral proteins, such as HIV-1 gp120 and Tat, affect the integrity of synaptic architecture and neuronal function (e.g., loss of

dendrites, alterations in mitochondrial metabolism (Bellizzi *et al*, 2005), leading eventually to neuronal apoptosis.

Phosphatidylinositol (PI) 3-kinase and Akt protein kinase play a role in the regulation of cell survival, including the survival of neurons (Crowder and Freeman, 1998; Dudek *et al*, 1997; Miller *et al*, 1997; Yao and Cooper, 1995). Glycogen synthase kinase (GSK)-3 β has been identified as a major physiological target for Akt (Cross *et al*, 1995), and GSK-3 β has been directly implicated in the regulation of apoptosis (Grimes and Jope, 2001, Sanchez *et al*, 2003). Our group has shown that candidate HIV-1 neurotoxins platelet-activating factor (PAF) and Tat activate GSK-3 β (Maggirwar *et al*, 1999) and lithium (an inhibitor of GSK-3 β) protects neurons against viral protein-induced cell death. Moreover, we have demonstrated that, in a mouse model of HIV-1 encephalitis, lithium can protect against virus-associated neurodegeneration (Dou *et al*, 2005). In this model, lithium protected against virus-infected macrophage-induced deficits in synaptic transmission, dendritic simplification, and neuronal loss (Dou *et al*, 2005). As mentioned above, one potential explanatory mechanism involves the manufacture and release of PAF from virus-infected MPs. Indeed, PAF leads to GSK-3 β activation, and its neurotoxic effects can be reversed by GSK-3 β inhibition (Maggirwar *et al*, 1999). This is particularly important, as PAF receptor activation can affect neuronal dysfunction and death mediated by candidate HIV-1 neurotoxins, including tumor necrosis factor alpha (TNF- α) (Perry *et al*, 1999).

The results of these studies provide a strong rationale to pursue human clinical trials. Furthermore, results of a recent small pilot study (Letendre *et al*, 2006) suggest that lithium may be beneficial in HIV-1-infected individuals with cognitive impairment. We have conducted a pilot study to investigate the safety and tolerability of lithium in individuals with HAND, and to provide additional preliminary data on the potential clinical benefit of lithium in this population using a multi-imaging modality approach.

Results

Subject demographic and clinical characteristics are summarized in Table 1. Participants were predominantly male (67%) and Caucasian (60%), with a mean age of 47 years. At baseline, 60% had a plasma HIV viral load in the undetectable range (≤ 50 copies/ml).

Of the 15 subjects enrolled, one elected to terminate treatment 6 days prior to the final visit date, in order to relocate to a different state. Data for this patient are included in both baseline and week 10 analyses. Two patients were discontinued from

Table 1 Baseline demographics and clinical characteristics

Age (years)	47.47(5.54)
Gender (% male)	66.67%
Race: N (% N)	
Caucasian	9 (60%)
African American	6 (40%)
Ethnicity: N (% N)	
Hispanic	2 (13.33%)
Non-Hispanic	13 (86.67%)
Education (years)	11.2 (1.42)
Years HIV+	12.1 (5.39)
CD4+ count: cells/mm ³	329.33 (207.11)
Plasma HIV RNA: N (% N)	
≤ 50 copies/ml	9 (60%)
> 50 , < 10000 copies/ml	5 (33.33%)
≤ 10000 copies/ml	1 (6.67%)
Karnofsky scale score: N (% N)	
80	7 (46.67%)
90	5 (33.33%)
100	3 (20%)
UPDRS Motor scale score	2.87 (3.68)

Note. Values are mean (standard deviation) unless otherwise indicated.

the study by the investigator: one after missing consecutive study visits and one due to a mild adverse event (atrioventricular [AV] block) associated with lithium therapy. This patient experienced vomiting and an elevated serum lithium level (1.35 mmol/L) at week 1, and lithium dose was reduced to 300 mg daily. Vomiting resolved, and serum lithium level at week 2 was 0.49 mmol/L; however, this patient also experienced AV block, which led to discontinuation of lithium and resolution of the AV block. One additional subject experienced vomiting at week 6 with a serum lithium level of 0.81 mmol/L; lithium dose was reduced to once per day for the remainder of the study and vomiting resolved. One subject experienced thyroid stimulating hormone (TSH) levels > 1.5 times the upper limit of normal at week 6 whereas lithium levels were < 0.5 mmol/L; lithium dosing was reduced to once per day, but TSH levels increased even after discontinuation of lithium and returned to normal only after initiating thyroid hormone replacement.

In summary, 13 of the 14 subjects (93%) who complied with study visits were able to stay on lithium throughout this 10-week study and dose adjustments were necessary only in two of these subjects; therefore, 11 of the 14 subjects (79%) completed the study at the originally assigned dose, exceeding the primary outcome of 50% tolerability ($P = .029$). There were no other significant laboratory changes at week 10 relative to baseline in any subjects. No significant clinical or statistical changes in CD4⁺ (mean CD4⁺ count decreased from 329.33/mm³ to 270.0/mm³) or viral load (mean viral load decreased from 6788.2 copies/ml to 4852.0 copies/ml) occurred from baseline to week 10. Week

10 lithium levels in patients who completed the study at the originally assigned dose ranged from 0.16 to 0.81 mmol/L, with a median value of 0.42 mmol/L.

Cognitive performance did not improve significantly from baseline to week 10 (Table 2), although the overall trend in the total neuropsychological (NP) z-score was toward improvement after lithium treatment. High levels of depressive symptoms, as measured by the CES-D¹ were present at baseline (Table 2); these values did not change significantly after 10 weeks of treatment with lithium. There were no significant changes in fatigue or subject global assessment of functioning; investigator global assessment of functioning indicated mild improvement in 69% of subjects and no change in 31%.

MRS

Concentrations of the metabolites *N*-acetyl aspartate (NAA), choline (Cho), *myo*-inositol (MI), the combined glutamate+glutamine (Glx) peak, and the internal reference Creatine (Cr) were determined in the three ROIs defined above, and ratios of each metabolite of interest to Cr were calculated. Changes in MRS metabolite ratios are reported in Table 3. A decrease in Glx/Cr was observed in the mid frontal gray matter ($P < .03$).

DTI

No significant changes in the DTI parameters of FA and MD in MRS regions of interest were observed. Nine subjects completed imaging at both baseline and week 10, and were included in the VBM analysis of DTI data. Comparisons using an uncorrected P value of .001 and a cluster size threshold of 5 revealed several areas of increased FA and decreased MD (Figure 1) that were not captured in the ROI analysis. FA increases were seen in gray matter areas including the right cerebellum, right basal ganglia and right frontal lobe (Figure 1a) whereas decreases in MD were present in the frontal lobes, right occipital lobe, and left globus pallidus (Figure 1b). Moreover, by superimposing DTI-VBM results with labeled major white matter tract atlases in stereotaxic space (Hua *et al*, 2008; Mori *et al*, 2008), we have identified increased FA in the forceps minor and external capsule as well as decreased MD in the anterior thalamic radiation (part of the anterior limb of the internal capsule).

fMRI

Activation patterns were compared in seven subjects with usable functional imaging data before and after lithium treatment. Results from the three-switch versus one-switch contrast (greatest attentional demand versus least attentional demand) are

Table 2 Neuropsychological and functional changes

	Baseline	Week 10	P value
Rey Auditory Verbal			
Memory (number correct)			
Total	32.47 (6.01)	37.14 (6.89)	.224
Trial 5	8.33 (2.26)	9.64 (2.17)	.089
Recall after	6.33 (2.02)	5.93 (1.69)	.398
Interference			
Delayed Recall	5.73 (2.25)	5.54 (1.81)	.556
Digit Symbol	39.27 (9.50)	40.00 (8.99)	.760
(number correct)			
Mean Reaction			
Time (ms)			
Choice	421.00 (38.20)	443.07 (48.81)	.033
Sequential	558.80 (150.77)	587.86 (162.80)	.357
Grooved Pegboard (s)			
Dominant Hand	77.07 (7.90)	73.57 (12.57)	.196
Non-dominant	83.07 (12.02)	80.64 (13.99)	.504
Hand			
Timed Gait (s)	8.64 (0.79)	8.05 (0.74)	.227
Neuropsychological	0.62 (3.15)	2.32 (3.38)	.635
z-score			
CES-D score	47.20 (10.95)	44.71 (12.05)	.486
FSS score	4.62 (1.63)	4.95 (1.62)	.596

Note. Values are mean (SD).

presented in Figure 2; the three-switch versus two-switch and two-switch versus one-switch contrasts showed similar but less prominent trends. To further assess the relevance of lithium-induced changes in activation patterns, fMRI data were compared with those from an age-matched group of HIV-infected cognitively normal subjects (Figure 2). MNI coordinates of peak (lowest P value) differences within clusters are presented in Table 4. Compared to HIV+ control subjects, subjects before treatment with lithium demonstrated significantly less activation during task performance in the bilateral superior temporal gyrus, bilateral cingulate, left precentral gyrus, left inferior frontal gyrus, and left superior frontal gyrus. Following lithium treatment, cognitively impaired subjects demonstrated significantly greater activation in a region extending from the left inferior to left superior temporal gyrus, as well as the left postcentral gyrus. Furthermore, after treatment with lithium, no significant differences in activated areas were detectable between HIV-infected subjects with cognitive impairment and cognitively normal HIV-infected subjects.

Conclusions

The results of this 10-week pilot open-label study indicate that lithium was tolerated by 93% of subjects with HIV-associated cognitive impairment, with 79% of subjects tolerating the maximum dose of 300 mg twice daily. Only one subject was discontinued early because of the occurrence of AV

¹ See Methods for definition of this and additional acronyms and abbreviations.

Table 3 Changes in MRS metabolites from baseline to week 10

		GMR <i>N</i> = 9*	95% confidence interval	<i>P</i> value
NAA/Cr	Centrum semi-ovale	1.042	(0.97,1.118)	.222
	Basal ganglia	1.017	(0.902, 1.147)	.756
	Mid-frontal gray matter	0.954	(0.811, 1.121)	.509
Cho/Cr	Centrum semi-ovale	1.017	(0.96, 1.077)	.525
	Basal ganglia	1.039	(0.95,1.136)	.357
	Mid-frontal gray matter	1.016	(0.9, 1.147)	.763
MI/Cr	Centrum semi-ovale	0.931	(0.827,1.047)	.197
	Basal ganglia	1.02	(0.739, 1.408)	.891
	Mid-frontal gray matter	0.949	(0.855, 1.054)	.276
Glx/Cr	Centrum semi-ovale	1.065	(0.906, 1.251)	.397
	Basal ganglia	1.243	(0.941, 1.643)	.109
	Mid-frontal gray matter	0.915	(0.848, 0.987)	.027

*One subject did not have usable MRS data in the basal ganglia at both time points; basal ganglia metabolites *N* = 8. GMR: geometric mean ratio.

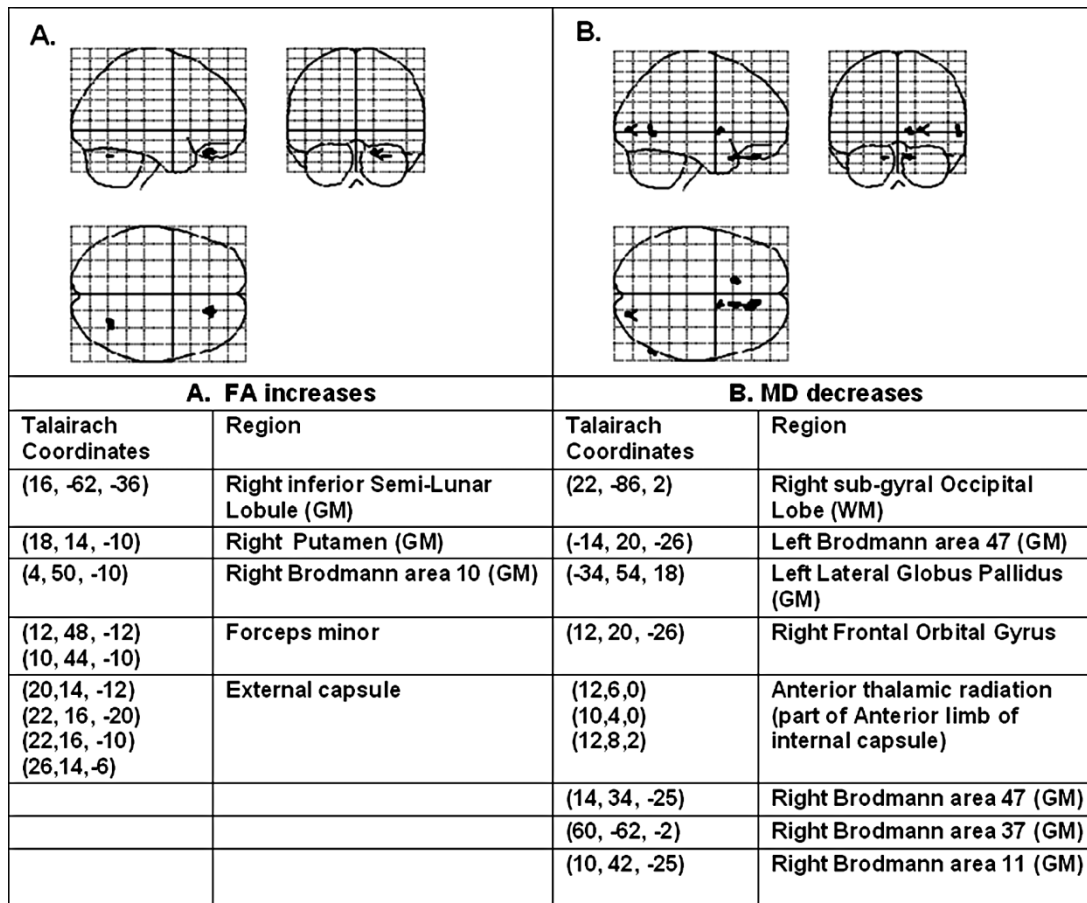


Figure 1 Areas of significant increases in FA (A) and decreases in MD (B) from baseline to week 10; uncorrected *p* = 0.001, cluster size threshold = 5.

block that resolved after stopping lithium. Two subjects (one because of vomiting and the other because of elevated TSH) completed the study at a reduced dose (300 mg/day). It is unclear whether the elevated TSH was lithium-induced, but mitigating against this, TSH levels were high at relatively low serum levels of lithium and continued to increase after stopping lithium. This patient was eventually

treated with thyroid hormone replacement and TSH serum levels normalized. There were no other changes in laboratory indices, including CD4⁺ count and viral load, observed during the 10-week treatment with lithium.

Secondary outcome measures in this study evaluated the effect of lithium on cognitive and functional performance, mood, and neuroimaging

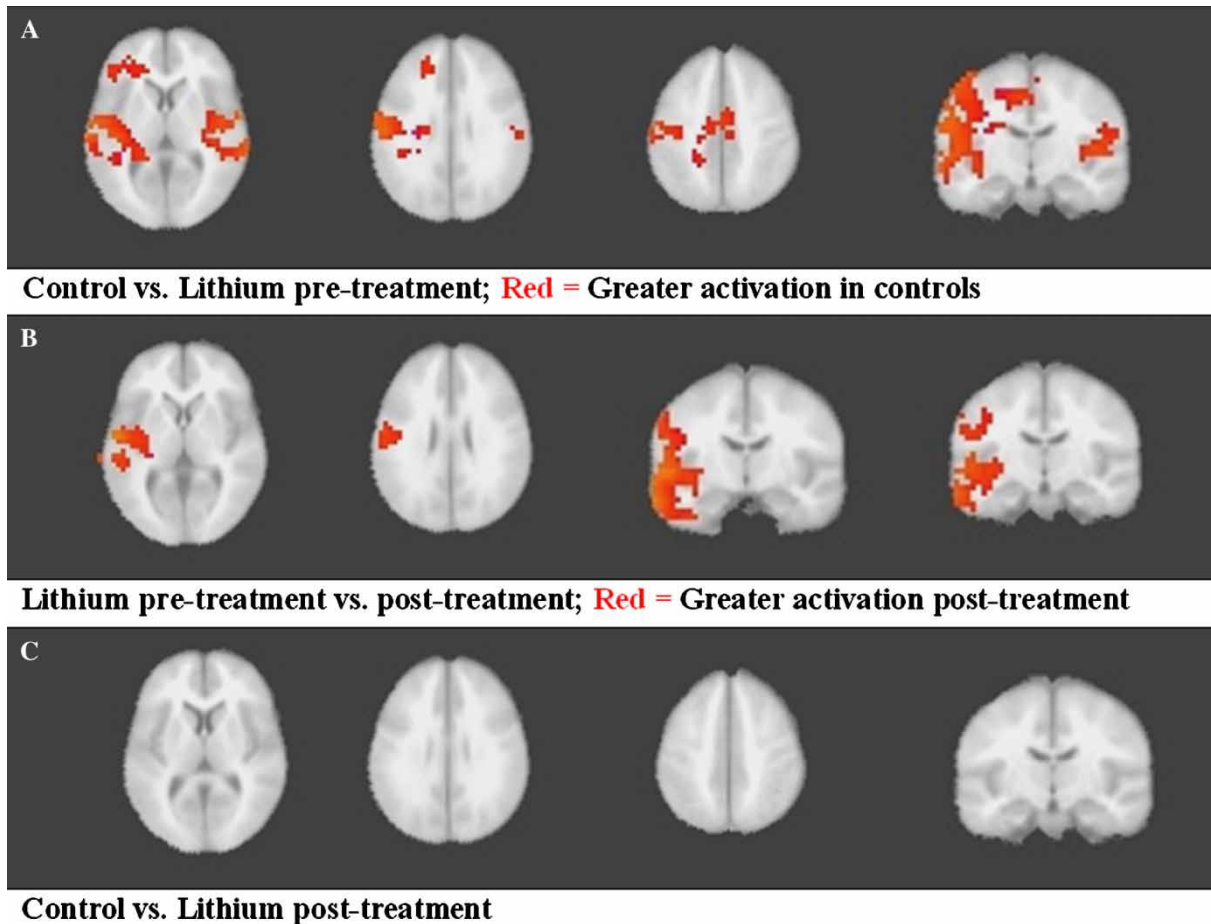


Figure 2 Between group differences in fMRI activation patterns. (A) Lithium subjects at baseline vs. HIV control subjects (B) Lithium subjects at baseline vs. 10 weeks (C) Lithium subjects at 10 weeks vs. HIV control subjects

biomarkers. Although no improvement was found in depressive symptoms, as measured by the CES-D score, or in subject global impression of function, investigator global impression, referencing global assessment of functioning described on p.7, lines 480–482. In contrast to the pilot study reported by Letendre *et al* (2006), we found only a trend toward improvement in cognitive performance. It should be noted that the two studies used different

cognitive outcomes and lithium dosing strategy, although the average dose and lithium levels achieved were comparable. Most importantly, both studies were pilot studies, with eight patients in Letendre *et al* (2006) and 13 subjects with usable data in this study. Furthermore, given the short duration of the current study, only a symptomatic effect on cognitive performance could be expected.

Table 4 fMRI cluster locations for areas of significantly different activation

Comparison	Region	Cluster peak coordinates	<i>P</i> value
(A) Control vs. lithium pretreatment	Left superior temporal gyrus	−57, −8, 4	.0005
	Right superior temporal gyrus	48, −13, 4	.0004
	Left inferior frontal gyrus	−42, 37, 6	.0002
	Left cingulate	−8, −16, 43	.0002
	Right cingulate	6, −8, 43	.0002
	Left precentral gyrus	−42, −19, 43	.0002
		−59, −12, 28	.0006
	Right postcentral gyrus	61, −22, 27	.0002
	Left superior frontal gyrus	−22, 38, 30	.0002
(B) Lithium pre- vs. post-treatment	Left superior temporal gyrus	−57, −8, 2	.0009
	Left poscentral gyrus	−55, −14, 25	.0004
	Left inferior temporal gyrus	−61, −9, −27	.0021
	Left middle temporal gyrus	−55, −12, −10	.0004

We hypothesized that neuroimaging biomarkers (MRS, DTI, and fMRI) would provide an early signature of lithium's disease-modifying activity that could be used to anticipate the appearance of clinical improvement. We have successfully implemented MRS in previous clinical trials and have found concordance between changes in brain metabolites and cognitive performance (Schiffitto *et al*, 2006, 2007a,b). In this study, we found a trend toward a decrease in glutamate + glutamine (Glx)/Cr concentration in the frontal gray matter whereas none of the other metabolites changed significantly. These results are consistent with recent reports of decreased Glx in multiple brain regions in normal volunteers and in patients with bipolar disorders (Friedman *et al*, 2004; Shibuya-Tayoshi *et al*, 2008) exposed to lithium. Shibuya-Tayoshi *et al* (2008) measured brain metabolites via MRS before and after 2 weeks of lithium administration in eight healthy subjects and found a significant decrease of Glx in the right basal ganglia and a trend in the left basal ganglia. Friedman *et al* (2004) have also assessed the impact of lithium on brain metabolites. Their study included 12 patients with bipolar disorder evaluated before starting lithium and after an average of 3.6 months, and 12 healthy controls. The investigators found a trend toward a decreased Glx in the gray matter of a brain region that included frontal, parietal, and occipital lobes and basal ganglia (slice centered on the anterior cingulate). Because elevated Glx concentrations have been reported in bipolar disorder (Yildiz-Yesiloglu and Ankerst, 2006), lithium-induced decreases in Glx may be part of its therapeutic mechanism.

More relevant to this study is the role that HIV-1-induced derangement of glutamate (Glu) metabolism may play in neuronal excitotoxicity. Previous investigations have shown that lithium modulates ionotropic Glu receptors, protecting neurons against Glu excitotoxicity (Du *et al*, 2004; Hashimoto *et al*, 2002; Nonaka *et al*, 1998). It has been suggested that HIV proteins and cytokines released by activated or infected microglia/macrophages interfere with astrocytic glutamate reuptake, thus increasing synaptic glutamate concentration, which can lead to neuronal excitotoxicity (Kaul *et al*, 2001). Therefore, modulation of Glu receptors by lithium may positively affect neuronal function. In vivo measures of Glx in HIV-infected patients with cognitive impairment have shown no significant increases in an earlier MRS study (Chang *et al*, 1999), whereas a decrease in Glx in the frontal white matter was reported recently (Sacktor, 2006). It should be noted that compartmental differences in brain metabolites are likely to occur and this could be reflected in a differential response to therapeutic intervention. For example Friedman *et al* (2004) found that Glx tended to increase after lithium treatment in the white matter, whereas Glx tended to decrease in the gray matter. It should be noted that a decrease in glial reuptake of glutamate

could also lead to decreased neuronal glutamate. Neurons require a glutamate-glutamine cycle that involves glial reuptake of glutamate from the synaptic clefts, which is then converted into glutamine. Glutamine released by glia reenters neuronal cells where it is converted into glutamate (Gruetter *et al*, 2003). This high-rate glutamate-glutamine cycling has been well documented using MRS (Sibson *et al*, 2001; Gruetter *et al*, 2003).

We investigated CNS microstructure using DTI (Mori and Zhang, 2006). A region of interest (ROI) approach, in the same regions investigated by MRS, did not show any significant changes before and after lithium administration. However, the voxel-based morphometry (VBM) analysis revealed several areas of increased FA and decreased MD after treatment with lithium (Figure 1). Some of these areas include the frontal lobes and white matter tracts, including the forceps minor and the external and internal capsules. It is noteworthy that a recent report has shown increases in frontal lobe gray matter volume and total white matter volume using a VBM approach in healthy volunteers after 4 weeks of lithium supplementation (Monkul *et al*, 2007).

We also employed fMRI to investigate the effect of lithium on HIV-infected individuals with cognitive impairment. The task used for the fMRI protocol was aimed at eliciting activation in circuitry subserving executive functioning (Garavan *et al*, 2000), which is affected in HIV-associated cognitive impairment. Our results suggest that cognitively impaired individuals have less brain activation during this task in several brain areas that have been associated with executive function (Garavan *et al*, 2000) than HIV-infected individuals who are cognitively normal (Figure 2a). However, treatment with lithium tends to normalize these differences observed at baseline (Figure 2c). Unfortunately our control group did not have a second scan and only comparisons with baseline could be made, therefore a practice effect cannot be ruled out. There are several reports in the bipolar literature spanning the entire spectrum of no change, increased, and decreased activation after lithium dosing regimens (Phillips *et al*, 2008). Comparisons to these reports are difficult to make because of the use of different tasks and populations investigated.

This pilot study follows our previous severely compromised immunodeficiency (SCID) HIV encephalitis (HIVE) animal study (Dou *et al*, 2005) that suggested lithium may have a neuroprotective role in HIV-associated cognitive impairment. Our results suggest that lithium can be used safely in HIV-infected individuals with cognitive impairment. Furthermore, the neuroimaging results confirm previous reports in patients or normal volunteers showing that lithium can decrease Glx in the gray matter, and may affect the brain microstructure (increased FA and decreased MD), as well as beneficially affect brain activation.

Our study has several limitations that are typical of pilot studies and open-label design. The small sample size reflects the proof of concept design with several explorative analyses. The open-label design further limits the conclusions that can be drawn from the study; however, the neuroimaging results provide a less subjective interpretation of the data. Additionally, the successful implementation of multiple imaging modalities within a single clinical trial demonstrates both the feasibility of this approach and the potential utility of the use of multiple modalities to strengthen neuroimaging findings and generate clinically meaningful results. Taken together, the results of this study are encouraging and warrant further investigations of lithium as adjunctive treatment for HIV-associated cognitive impairment.

Methods

Subjects

Fifteen HIV-1-infected individuals with cognitive impairment (CI) were enrolled in this 10-week, open-label study at the University of Rochester CI was defined as (a) performance at least 1.0 standard deviation below age- and education-matched controls on two or more separate neuropsychological tests; and/or (b) performance at least 2.0 standard deviations below age-matched and education-matched controls on one or more separate neuropsychological tests. Normative data for neuropsychological test scores were the same as those used in the Dana and Northeast AIDS Dementia (NEAD) cohorts (Marder *et al*, 2003; Dana Consortium on Therapy for HIV Dementia and Related Cognitive Disorders, 1996). Participants were recruited from the NEAD cohort and Rochester AIDS Clinical Trials Unit (ACTU) HIV-infected population, and were required to be on a stable antiretroviral regimen or off antiretroviral therapy for at least 8 weeks prior to study entry. Patients were excluded if they were pregnant or breastfeeding, of reproductive potential and unwilling to use effective barrier birth control methods, or had active opportunistic acquired immunodeficiency syndrome (AIDS)-defining infections within 30 days of study entry; severe premorbid psychiatric illness likely to interfere with protocol compliance; confounding neurological disorders; a history of or current central nervous system (CNS) infection or neoplasms; or any other clinically significant condition or laboratory abnormality that, in the investigator's opinion would interfere with the individual's ability to participate in the study. Subjects with positive rapid plasma reagin (RPR) were not excluded from participation if CSF Venereal Dis-

ease Research Laboratory (VDRL) tests were negative.

Study design

The study was reviewed and approved by the Institutional Review Board at the University of Rochester Medical Center. All subjects signed a written informed consent prior to undergoing the screening evaluation. After informed consent was obtained and screening measures completed, subjects were instructed to begin taking lithium carbonate 300 mg PO bid at approximate 12-h intervals. The initial dose was administered by clinic staff at the baseline visit, and patients were observed for about 1 h. Follow-up evaluations were conducted at 1, 2, 4, 6, and 10 weeks after the baseline visit.

Procedures

Clinical assessments

At each visit, participants were assessed for adverse experiences. Clinical assessments performed at each visit included vital signs; updated diagnoses, signs and symptoms; the Karnofsky Performance Scale; and a pill count to assess medication compliance. A battery of safety surveillance laboratory tests, including serum chemistry profiles (electrolytes, uric acid, and liver function tests), hematology, and urine analysis, was performed at initial screening and at weeks 2, 6, and 10. Lithium serum levels were measured between 12 and 18 h post dose at weeks 1, 2, 4, 6, and 10. Women of childbearing potential were given a serum or urine pregnancy test at each visit. A neurological examination was performed and plasma HIV RNA (Roche Amplicor HIV-1 Monitor Ultrasensitive Method) and CD4⁺/CD8⁺ cell counts and percentages were measured at study entry, and week 10. An electrocardiogram was performed at the screening visit and at weeks 2, 6, and 10.

Neuropsychological/functional measures

Neuropsychological evaluations derived from the battery used by the Dana Consortium (Dana Consortium on Therapy for HIV Dementia and Related Cognitive Disorders, 1996) included the Rey Auditory Verbal Learning Test; Digit Symbol Test; Grooved Pegboard (dominant and non-dominant hands); Timed Gait; and the California Computerized Assessment Package (CalCAP) reaction time test. Subjects completed neuropsychological assessments at the screening visit, and weeks 6 and 10. Premorbid intellectual functioning was estimated at screening using the WAIS-R vocabulary test. Global assessments of functioning were completed by the subject and investigator at screening, week 6, and week 10, along with assessments of fatigue, using the Fatigue Severity Scale (Krupp *et al*, 1989) and mood, using

the Center for Epidemiologic Studies Depression Scale.

Neuroimaging

All magnetic resonance (MR) images were acquired on a Siemens 3T Trio system with an 8-channel head coil. Sagittal 3D T₁W images were collected using an MP-RAGE sequence with TR/TE/TI = 2530/3.39/1100 ms, 1 average, 1 mm slice thickness, FOV = 256 × 256 × 160 mm, an acquisition matrix of 192 × 256 × 160 with zero filling to generate a final imaging matrix of 256 × 256 × 160 and image resolution of 1 × 1 × 1 mm, 1 NEX. Proton density and T₂W images were acquired using a double-echo sequence with the following parameters: TE1/TE2/TR = 8.9/143/4000, 2.5 mm interleaved slices, FOV = 23 cms, matrix size = 256 × 256, 1 average.

MRS. Single-voxel proton spectra were acquired using a PRESS sequence from three different locations in the brain: midline of the frontal lobes (gray matter [GM]), right (or left) mid-frontal centrum semi-ovale (white matter [WM]), and right (or left) basal ganglia (deep GM). Voxels 20 × 20 × 20 mm³ were prescribed graphically from the proton density axial images acquired during the same examination. TR/TE = 2000/30 ms, 96 averages, and spectral width of 1000 Hz were used for each voxel. Metabolite concentrations were determined with LCModel software (version 6.1) (Provencher, 1993, 2001), which analyzes the spectra as a linear combination of a set of model spectra of metabolite solutions in vitro. For all spectroscopic data, the reference basis set for 3-Tesla PRESS sequence with TE = 30 ms was used. All spectral fits were performed in an analysis window from 1 to 4.0 ppm. Metabolite concentrations with uncertainties (Cramer-Rao lower bounds) larger than 20%, as given by LCModel, were not included in the statistical analysis. An unsuppressed water reference signal was combined with water-suppressed data to estimate absolute metabolite concentrations.

DTI DTI data were acquired with TR/TE = 10100/100 ms, isotropic 2 × 2 × 2 mm voxel size, image matrix = 128 × 128, iPAT (GRAPPA) acceleration factor = 2, 24 diffusion gradient directions with b = 1000s/mm² and one average, b = 0 images with 4 averages. Double-echo GRE images were also acquired for the purpose of field mapping, and the abovementioned high-resolution 3D MP-RAGE T₁W images were used for spatial normalization. A custom software package developed in C++ and Matlab (The Mathworks, Natick, MA) as well as the public domain image processing tools listed below were used in the post processing and statistical analysis. Values of mean diffusivity (MD) and fractional anisotropy (FA) were tabulated for all voxels contained within regions of interest (ROI) measured in MRS acquisition, and averaged to produce a mean value for MD and FA for each ROI. A whole-brain voxel based morphometry

(VBM) approach was implemented to explore additional brain areas that may have been affected by lithium treatment.

All DTI data of each subject went through four processing steps before statistical analysis: (a) Eddy current distortion and intraprotocol subject motion correction, (b) field-map based susceptibility artifacts correction, (c) calculation of the diffusion tensor, and (d) spatial normalization of tensor data. Eddy current artifacts as well as subject movement artifacts among different gradient encoding directions within the same DTI scan were first simultaneously removed using a model-based geometric distortion correction method (Andersson and Skare, 2002). Geometric distortions in DTI-EPI images caused by magnetic field heterogeneity were corrected using the FieldMap toolbox provided by the SPM2 package (<http://www.fil.ion.ucl.ac.uk/spm/toolbox/fieldmap/>). A linear ordinary least squares (OLS) fit was then performed to obtain the initial estimation of the diffusion tensor. During this procedure, nonbrain structures were removed using the FSL Brain Extraction Tool (<http://www.fmrib.ox.ac.uk/fsl/bet2/>; FMRIB Analysis Group, Oxford University, UK).

Spatial normalization based on the SPM2 package (The Wellcome Department of Imaging Neuroscience, University College London) was performed on the DTI data sets by a two-stage process: a 12-degree of freedom affine registration between the non-DW images and the T₁W images of each subject followed by a nonlinear registration between individual T₁W images and the MNI152 T₁ GM + WM template (Montreal Neurological Institute, Canada). For the second stage, an optimized routine similar to the optimized VBM approach (Good *et al*, 2001) was used. In brief, each subject's MP-RAGE T₁W image was segmented into GM/WM/CSF using SPM2 segmentation tools. After segmentation, each subject's GM + WM image was spatially normalized to the MNI152 T₁ GM + WM template using a nonlinear registration algorithm from SPM2. Finally, the jointed transformation matrix from the aforementioned two stages was applied to the tensor data for the VBM analysis. To minimize the potential bias from CSF, a global GM + WM mask was generated as the explicit mask for VBM analysis by combining GM + WM masks from all subjects with a logic AND operation. Additionally, the preservation of principal direction algorithm (Alexander *et al*, 2001) was applied to the calculated tensor data to compensate for the disturbances in tensor orientations caused by spatial normalization.

fMRI All subjects were administered a working memory and executive function task. The task was based on Garavan *et al* (2000) and consisted of visually presented sequences of large and small squares intermixed with fixation trials. Participants were required to retain in memory separate counts of small and large squares. The number of switches

between square sizes was varied between trials (one, two, or three switches) while the memory demands (total number of squares) were held constant. Participants were told to silently verbally rehearse the results during stimulus presentation. At the end of each trial, the subject was asked to press a button indicating whether they had seen more large or small squares. To avoid practice effects, the length of each of the five runs in each scan was varied between 11 to 15 squares in a random order. There were three runs for a total of 195 squares. Each run was considered a condition (one-, two-, or three-switch) based on the number of times the size of squares was changed. Prior to scanning, all subjects completed a brief training session to ensure comprehension of the task.

Contiguous 4-mm axial slices were obtained during task performance using the following parameters: GRE EPI pulse sequence with TR/TE = 2000/30 ms, $4 \times 4 \times 4$ mm voxel size, 64×64 matrix. Using AFNI software (Cox, 1996), slice timing correction was performed as well as correction for head movement using a rigid body (6-parameter) transformation. Subjects who exhibited more than 2 mm of head movement in any direction were discarded from subsequent analysis. Next, using FSL software (<http://fmrib.ox.ac.uk/fsl>), each subject's images were skull-stripped, normalized to MNI space (Montreal Neurological Institute, Canada), and spatially smoothed with a Gaussian kernel of full width at half maximum (FWHM) of two times the voxel dimension (8 mm).

Statistical analyses were performed using AFNI software. Three contrasts of interest were examined using the general linear model: two-switch versus one-switch, three-switch versus two-switch, and three-switch versus one switch. To identify regions that differed in activation across groups of patients, the AFNI program 3dWilcoxon was used to perform the Wilcoxon signed-rank test for paired data sets (to compare subjects before and after lithium treatment) and Wilcoxon signed-rank test for unpaired data sets (to compare HIV cognitively normal subjects to HIV cognitively impaired subjects before and after lithium treatment), yielding a normalized Wilcoxon statistic for each voxel. Multiple comparison corrections were done using a cluster size approach: clusters with a corrected P

value $< .05$ and containing at least 128 voxels were considered significant.

Outcome measures

The primary measure of tolerability in this study was the proportion of subjects who completed the full 10 weeks of treatment at the originally assigned dose of experimental medication. Safety measures included the incidence of adverse experiences and abnormal laboratory tests. Measures of efficacy included neuropsychological test scores, MRI indices, and changes in functioning and mood.

Statistical methods

The study was designed to provide 85% power to detect whether more than 50% of the patients were able to tolerate the full dose of experimental medication using a one-sided exact binomial test at the .05 level of significance. Neuropsychological test scores and measures of fatigue (fatigue severity scale [FSS]) (Krupp *et al*, 1989), mood (Center for Epidemiology Studies Depression Scale [CES-D]) (Radloff, 1977) and subject global assessment of functioning were compared using paired t tests of the changes from baseline to week 10. Relative changes in MRS and DTI ROI values were assessed using paired t tests of the changes from baseline to week 10 on the log scale, and these mean changes and associated 95% confidence intervals were back-transformed to the original scale, where they correspond to geometric mean ratios. Paired Wilcoxon signed rank tests were used to compare $CD4^+$, and other laboratory values from baseline to week 10. No adjustments for multiple comparisons were applied for the 12 neuropsychological comparisons, the 12 MRS comparisons, or the laboratory tests because interest was primarily focused on the single test of the neuropsychological z-score, magnetic resonance spectroscopy (MRS) analyses were exploratory, and reducing power to detect changes in laboratory values is inappropriate for safety monitoring. The statistical approach for fMRI and VBM analyses is described above.

Declaration of interest: The authors report no conflicts of interest. The authors alone are responsible for the content and writing of the paper.

References

- Alexander DC, Pierpaoli C, Basser PJ, Gee JC (2001). Spatial transformations of diffusion tensor magnetic resonance images. *IEEE Trans Med Imaging* **20**: 1131–1139.
- Andersson JL, Skare S (2002). A model-based method for retrospective correction of geometric distortions in diffusion-weighted EPI. *Neuroimage* **16**: 177–199.
- Antinori A, Arendt G, Becker JT, Brew BJ, Byrd DA, Cherner M, Clifford DB, Cinque P, Epstein LG, Goodkin K, Gisslen M, Grant I, Heaton RK, Joseph J, Marder K, Marra CM, McArthur JC, Nunn M, Price RW, Pulliam L, Robertson KR, Sacktor N, Valcour V, Wojna VE (2007). Updated research nosology for HIV-associated neurocognitive disorders. *Neurology* **69**: 1789–1799.
- Bellizzi MJ, Lu SM, Masliah E, Gelbard HA (2005). Synaptic activity becomes excitotoxic in neurons

- exposed to elevated levels of platelet-activating factor. *J Clin Invest* **115**: 3185–3192.
- Chang L, Ernst T, Leonido-Yee M, Walot I, Singer E (1999). Cerebral metabolite abnormalities correlate with clinical severity of HIV-1 cognitive motor complex. *Neurology* **52**: 100–108.
- Cox RW (1996). AFNI: software for analysis and visualization of functional magnetic resonance neuroimages. *Comput Biomed Res* **29**: 162–173.
- Cross DA, Alessi DR, Cohen P, Andjelkovic M, Hemmings BA (1995). Inhibition of glycogen synthase kinase-3 by insulin mediated by protein kinase B. *Nature* **378**: 785–789.
- Crowder RJ, Freeman RS (1998). Phosphatidylinositol 3-kinase and Akt protein kinase are necessary and sufficient for the survival of nerve growth factor-dependent sympathetic neurons. *J Neurosci* **18**: 2933–2943.
- Dana Consortium on Therapy for HIV Dementia and Related Cognitive Disorders (1996). Clinical confirmation of the American Academy of Neurology algorithm for HIV-1-associated cognitive motor disorder. *Neurology*, **47**: 1247–1253.
- Dou H, Ellison B, Bradley J, Kasiyanov A, Poluektova LY, Xiong H, Maggirwar S, Dewhurst S, Gelbard HA, Gendelman HE (2005). Neuroprotective mechanisms of lithium in murine human immunodeficiency virus-1 encephalitis. *J Neurosci* **25**: 8375–8385.
- Du J, Gray NA, Falke CA, Chen W, Yuan P, Szabo ST, Einat H, Manji HK (2004). Modulation of synaptic plasticity by antimanic agents: the role of AMPA glutamate receptor subunit 1 synaptic expression 67. *J Neurosci* **24**: 6578–6589.
- Dudek H, Datta SR, Franke TF, Birnbaum MJ, Yao R, Cooper GM, Segal RA, Kaplan DR, Greenberg ME (1997). Regulation of neuronal survival by the serine-threonine protein kinase Akt. *Science* **275**: 661–665.
- Friedman SD, Dager SR, Parow A, Hirashima F, Demopoulos C, Stoll AL, Lyoo IK, Dunner DL, Renshaw PF (2004). Lithium and valproic acid treatment effects on brain chemistry in bipolar disorder. *Biol Psychiatry* **56**: 340–348.
- Garavan H, Ross TJ, Li SJ, Stein EA (2000). A parametric manipulation of central executive functioning. *Cerebral Cortex* **10**: 585–592.
- Glass JD, Wesselingh SL, Selnes OA, McArthur JC (1993). Clinical-neuropathologic correlation in HIV-associated dementia. *Neurology* **43**: 2230–2237.
- Good CD, Johnsrude IS, Ashburner J, Henson RN, Friston KJ, Frackowiak RS (2001). A voxel-based morphometric study of ageing in 465 normal adult human brains. *Neuroimage* **14**: 21–36.
- Grimes CA, Jope RS (2001). The multifaceted roles of glycogen synthase kinase 3 β in cellular signaling. *Prog Neurobiol* **65**: 391–426.
- Gruetter R, Adriany G, Choi IY, Henry PG, Lei H, Oz G (2003). Localized in vivo ¹³C NMR spectroscopy of the brain. *NMR Biomed* **16**: 313–338.
- Hashimoto R, Hough C, Nakazawa T, Yamamoto T, Chuang DM (2002). Lithium protection against glutamate excitotoxicity in rat cerebral cortical neurons: involvement of NMDA receptor inhibition possibly by decreasing NR2B tyrosine phosphorylation. *J Neurochem* **80**: 589–597.
- Hua K, Zhang J, Wakana S, Jiang H, Li X, Reich DS, Calabresi PA, Pekar JJ, van Zijl PC, Mori S (2008). Tract probability maps in stereotaxic spaces: analyses of white matter anatomy and tract-specific quantification. *Neuroimage* **39**: 336–347.
- Kaul M, Garden GA, Lipton SA (2001). Pathways to neuronal injury and apoptosis in HIV-associated dementia. *Nature* **410**: 988–994.
- Krupp LB, LaRocca NG, Muir-Nash J, Steinberg AD (1989). The fatigue severity scale. Application to patients with multiple sclerosis and systemic lupus erythematosus. *Arch Neurol* **46**: 1121–1123.
- Letendre SL, Woods SP, Ellis RJ, Atkinson JH, Masliah E, van den BG, Durelle J, Grant I, Everall I, Group HNRC (2006). Lithium improves HIV-associated neurocognitive impairment. *AIDS* **20**: 1885–1888.
- Maggirwar SB, Tong N, Ramirez S, Gelbard HA, Dewhurst S (1999). HIV-1 Tat-mediated activation of glycogen synthase kinase-3 beta contributes to Tat-mediated neurotoxicity. *J Neurochem* **73**: 578–586.
- Marder K, Albert SM, McDermott MP, McArthur JC, Schifitto G, Selnes OA, Sacktor N, Stern Y, Palumbo D, Kieburtz K, Cohen B, Orme C, Epstein LG (2003). Inter-rater reliability of a clinical staging of HIV-associated cognitive impairment. *Neurology* **60**: 1467–1473.
- Miller TM, Tansey MG, Johnson EM Jr, Creedon DJ (1997). Inhibition of phosphatidylinositol 3-kinase activity blocks depolarization- and insulin-like growth factor-I mediated survival of cerebellar granule cells. *J Biol Chem* **272**: 9847–9853.
- Monkul ES, Matsuo K, Nicoletti MA, Dierschke N, Hatch JP, Dalwani M, Brambilla P, Caetano S, Sassi RB, Mallinger AG, Soares JC (2007). Prefrontal gray matter increases in healthy individuals after lithium treatment: a voxel-based morphometry study. *Neurosci Lett* **429**: 7–11.
- Mori S, Oishi K, Jiang H, Jiang L, Li X, Akhter K, Hua K, Faria AV, Mahmood A, Woods R, Toga AW, Pike GB, Neto PR, Evans A, Zhang J, Huang H, Miller MI, van ZP, Mazziotta J (2008). Stereotaxic white matter atlas based on diffusion tensor imaging in an ICBM template. *Neuroimage* **40**: 570–582.
- Mori S, Zhang J (2006). Principles of diffusion tensor imaging and its applications to basic neuroscience research. *Neuron* **51**: 527–539.
- Nonaka S, Hough CJ, Chuang DM (1998). Chronic lithium treatment robustly protects neurons in the central nervous system against excitotoxicity by inhibiting N-methyl-D-aspartate receptor-mediated calcium influx. *Proc Natl Acad Sci U S A* **95**: 2642–2647.
- Perry SW, Hamilton JA, Tjoelker LW, Dbaibo G, Dzenko KA, Epstein LG, Hannun Y, Whittaker JS, Dewhurst S, Gelbard HA (1999). Platelet-activating factor receptor activation: an initiator step in HIV-1 neuropathogenesis. *J Biol Chem* **273**: 17660–17664.
- Phillips ML, Travis MJ, Fagiolini A, Kupfer DJ (2008). Medication effects in neuroimaging studies of bipolar disorder. *American Journal of Psychiatry* **165**: 313–320.
- Provencher SW (1993). Estimation of metabolite concentrations from localized in vivo proton NMR spectra. *Magn Reson Med* **30**: 672–679.
- Provencher SW (2001). Automatic quantitation of localized in vivo 1H spectra with LCModel. *NMR Biomed* **14**: 260–264.
- Radloff LL (1977). The CES-D: a self-report depression scale for research in the general population. *Appl Psychol Meas* **1**: 385–401.

- Sacktor N (2006). Magnetic resonance spectroscopy abnormalities using a 3.0 tesla field strength in individuals with HIV dementia. *Ann Neurol* **60 Suppl 3**: S24–S24.
- Sacktor N, McDermott MP, Marder K, Schifitto G, Selnes OA, McArthur JC, Stern Y, Albert S, Palumbo D, Kieburtz K, deMarcaida JA, Cohen B, Epstein L (2002). HIV-associated cognitive impairment before and after the advent of combination therapy. *J NeuroVirol* **8**: 136–142.
- Sanchez JF, Sniderhan LF, Williamson AL, Fan S, Chakraborty-Sett S, Maggirwar SB (2003). Glycogen synthase kinase 3 β -mediated apoptosis of primary cortical astrocytes involves inhibition of nuclear factor κ B signaling. *Mol Cell Biol* **23**: 4649–4662.
- Schifitto G, Navia BA, Yiannoutsos CT, Marra CM, Chang L, Ernst T, Jarvik JG, Miller EN, Singer EJ, Ellis RJ, Kolson DL, Simpson D, Nath A, Berger J, Shriver SL, Millar LL, Colquhoun D, Lenkinski R, Gonzalez RG, Lipton SA (2007a). Memantine and HIV-associated cognitive impairment: a neuropsychological and proton magnetic resonance spectroscopy study. *AIDS* **21**: 1877–1886.
- Schifitto G, Peterson DR, Zhong J, Ni H, Cruttenden K, Gaugh M, Gendelman HE, Boska M, Gelbard H (2006). Valproic acid adjunctive therapy for HIV-associated cognitive impairment: a first report. *Neurology* **66**: 919–921.
- Schifitto G, Yiannoutsos CT, Ernst T, Navia B, Sacktor N, Nath A, Clifford DB (2007b). Impact of selegiline transdermal system on measures of brain metabolism and markers of oxidative stress in HIV infected individuals with cognitive impairment. *J NeuroVirol* **13**: 122–123.
- Shibuya-Tayoshi S, Tayoshi S, Sumitani S, Ueno S, Harada M, Ohmori T (2008). Lithium effects on brain glutamatergic and GABAergic systems of healthy volunteers as measured by proton magnetic resonance spectroscopy. *Prog Neuropsychopharmacol Biol Psychiatry* **32**: 249–256.
- Sibson NR, Mason GF, Shen J, Cline GW, Herskovits AZ, Wall JE, Behar KL, Rothman DL, Shulman RG (2001). In vivo (13)C NMR measurement of neurotransmitter glutamate cycling, anaplerosis and TCA cycle flux in rat brain during. *J Neurochem* **76**: 975–989.
- Yao R, Cooper GM (1995). Requirement for phosphatidylinositol-3 kinase in the prevention of apoptosis by nerve growth factor. *Science* **267**: 2003–2006.
- Yildiz-Yesiloglu A, Ankerst DP (2006). Neurochemical alterations of the brain in bipolar disorder and their implications for pathophysiology: a systematic review of the in vivo proton magnetic resonance spectroscopy findings. *Prog Neuropsychopharmacol Biol Psychiatry* **30**: 969–995.

This paper was first published online on iFirst on 24 April 2009.